Supporting Information:

Future changes in isoprene-epoxydiol-derived secondary organic aerosol (IEPOX-SOA) under the shared socioeconomic pathways: the importance of explicit chemistry

Duseong S. Jo[1,2,3], Alma Hodzic[3], Louisa K. Emmons[3], Simone Tilmes[3], Rebecca H. Schwantes[3,#,△], Michael J. Mills[3], Pedro Campuzano-Jost[1,2], Weiwei Hu[1,2,*], Rahul A. Zaveri[4], Richard C. Easter[4], Balwinder Singh[4], Zheng Lu[5], Christiane Schulz[6,7], Johannes Schneider[6], John E. Shilling[4], Armin Wisthaler[8,9], and Jose L. Jimenez[1,2]

[1] Cooperative Institute for Research in Environmental Sciences (CIRES), University of Colorado, Boulder, CO, USA
[2] Department of Chemistry, University of Colorado, Boulder, CO, USA
[3] National Center for Atmospheric Research, Boulder, CO, USA
[4] Atmospheric Sciences and Global Change Division, Pacific Northwest National Laboratory, Richland, WA, USA
[5] Department of Atmospheric Sciences, Texas A&M University, College Station, Texas
[6] Particle Chemistry Department, Max Planck Institute for Chemistry, Mainz, Germany
[7] Leibniz Institute for Tropospheric Research, Leipzig, Germany
[8] Department of Chemistry, University of Oslo, Oslo, Norway
[9] Institute for Ion Physics and Applied Physics, University of Innsbruck, Innsbruck, Austria
[#]Now at: Cooperative Institute for Research in Environmental Sciences, University of Colorado, Boulder, CO, USA
[△]Now at: Chemical Sciences Laboratory, National Oceanic and Atmospheric Administration, Boulder, CO, USA
[*]Now at: State Key Laboratory of Organic Geochemistry, Guangzhou Institute of Geochemistry, Chinese Academy of Sciences, Guangzhou, China

Correspondence to: Duseong S. Jo (duseong.jo@colorado.edu)

1 Isoprene emission comparison

We compared the annual isoprene emissions for 2011–2013 simulated by CESM2.1.0/MEGANv2.1 and by OMI top-down estimate (Bauwens et al. 2016, available at: http://emissions.aeronomie.be/index.php/omi-based, last access: 1 March 2020). As shown in Figure S1c, CESM2.1.0/MEGANv2.1 overestimates isoprene emissions over the Tropics and underestimates them at high latitudes in the Northern Hemisphere. In terms of magnitude, isoprene emissions over the Tropics are important. We scaled down Tropical isoprene emissions by reducing emission factors of Tropical plant functional types (PFT). Two PFTs were used in the Community Land Model version 5 (CLM5): "broadleaf evergreen tropical tree" and "broadleaf deciduous tropical tree". These two PFTs contribute ~80% of total global isoprene emissions (Guenther et al. 2012). There were still regional discrepancies between CESM2.1.0/MEGANv2.1 and top-down estimates (Figures S1d and S1e), but the global total emission amount became closer to the total emission value by the OMI top-down estimate. Global total annual isoprene emissions changed from 439 Tg yr^{-1} to 260 Tg yr^{-1}, which was comparable to the top-down estimate (266 Tg yr^{-1}).

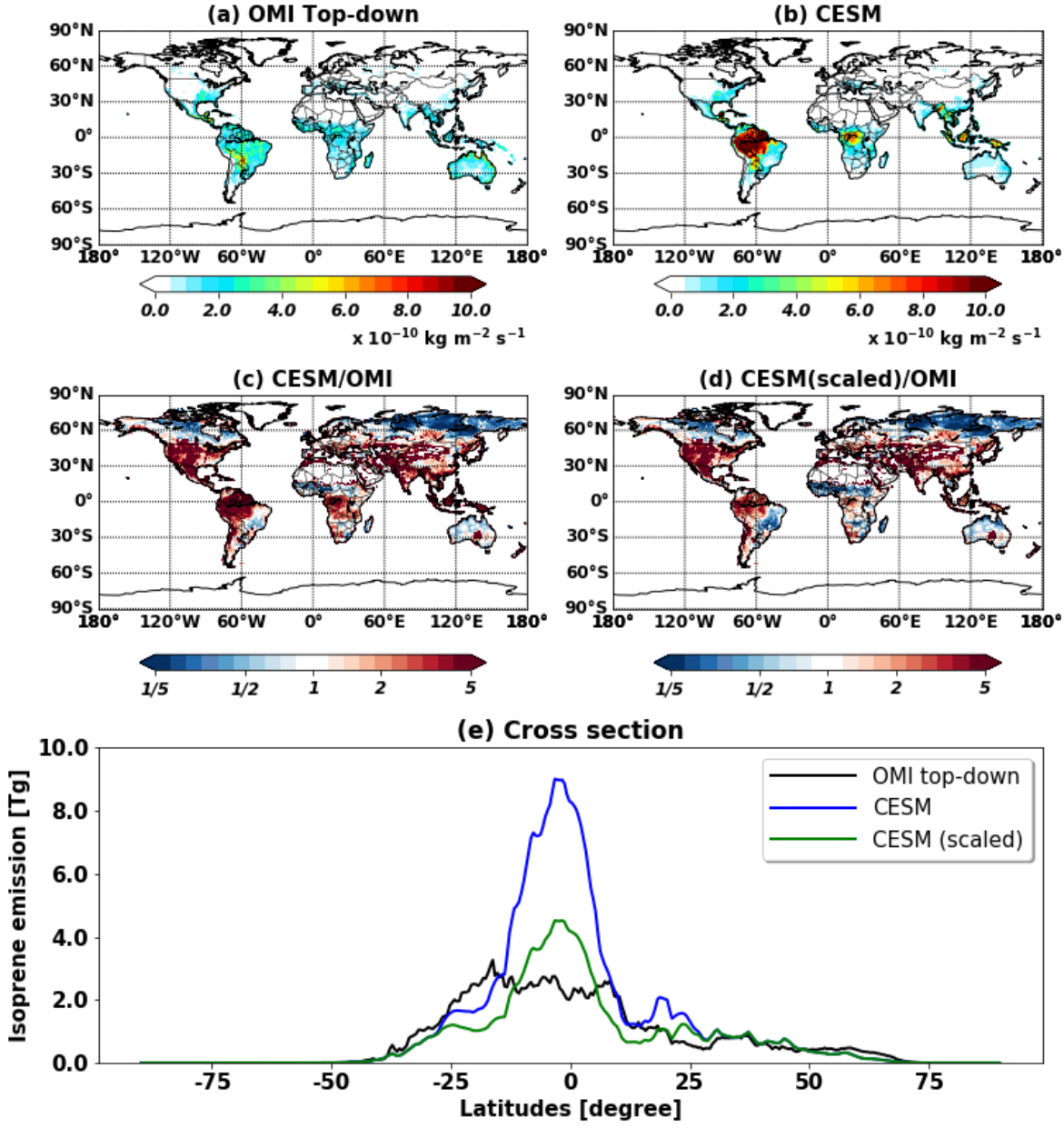

Figure S1. Annual isoprene emissions for 2011–2013 by (a) OMI top-down and (b) CESM2.1.0/MEGANv2.1. (c) Ratios of CESM2.1.0/MEGANv2.1 to OMI top-down isoprene emissions. (d) same as (c) but the isoprene emission factors of tropical trees in CESM2.1.0/MEGANv2.1 are reduced by 50%. (e) Zonal mean cross-section of annual isoprene emissions.

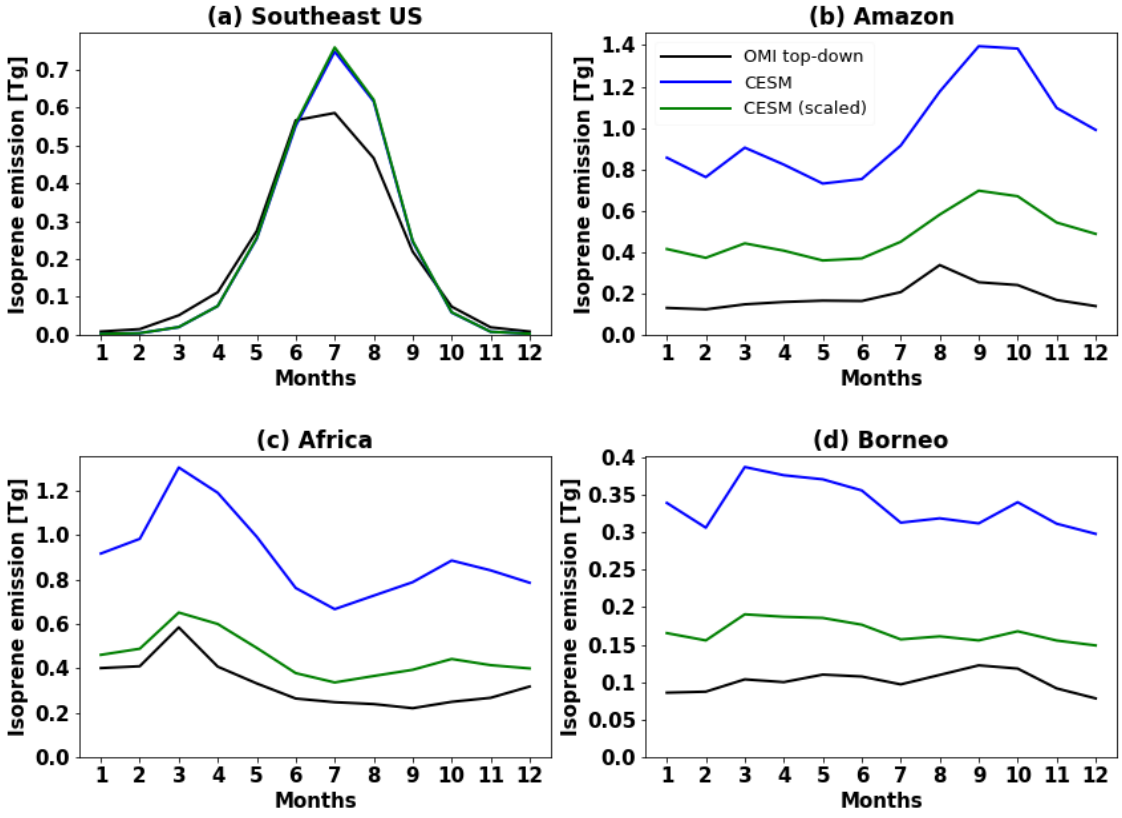

45

Figure S2. Time series of Isoprene emissions (2011–2013) over (a) Southeast US (30–40°N, 100–80°W), (b) Amazon (10–0°S, 70–60°W), (c) Africa (5°S–5°N, 10–30°E), and (d) Borneo (5°S–5°N, 105–120°E).

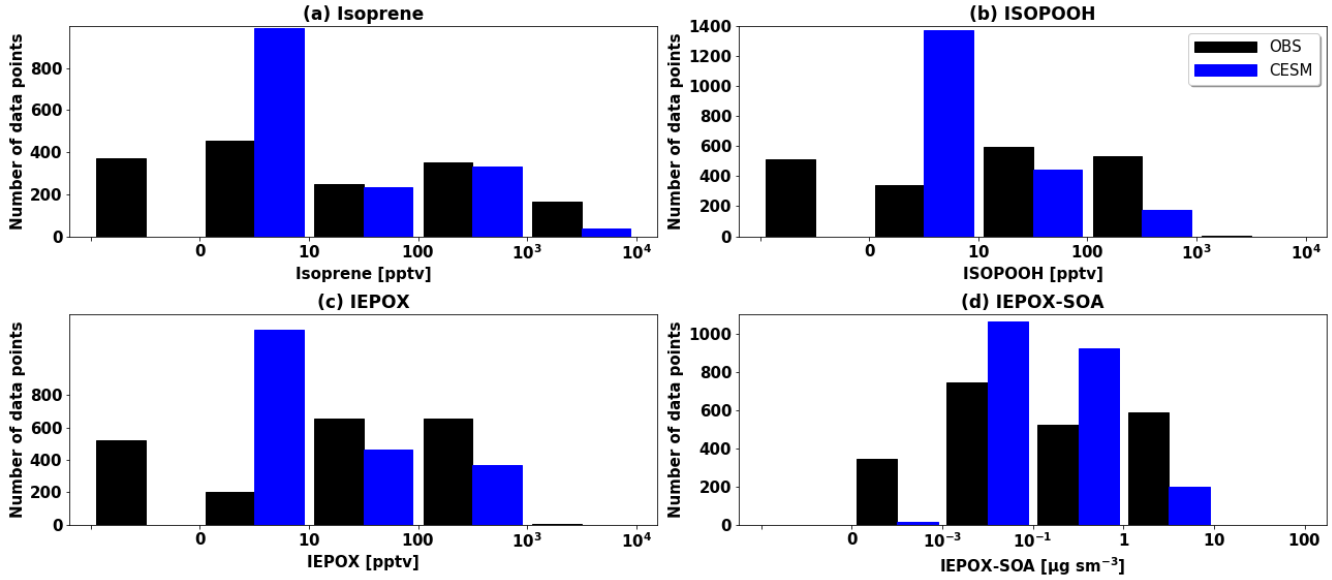

Figure S3. Histograms for observed and modeled (a) isoprene, (b) ISOPOOH, (c) IEPOX, and (d) IEPOX-SOA concentrations during the SEAC4RS campaign. Observation and model results are shown in black and blue bars, respectively. We note that gas measurements can be negative when the real concentrations are zero or very low due to instrumental noise. On the other hand, IEPOX-SOA concentrations were calculated by the positive matrix factorization method and always positive.

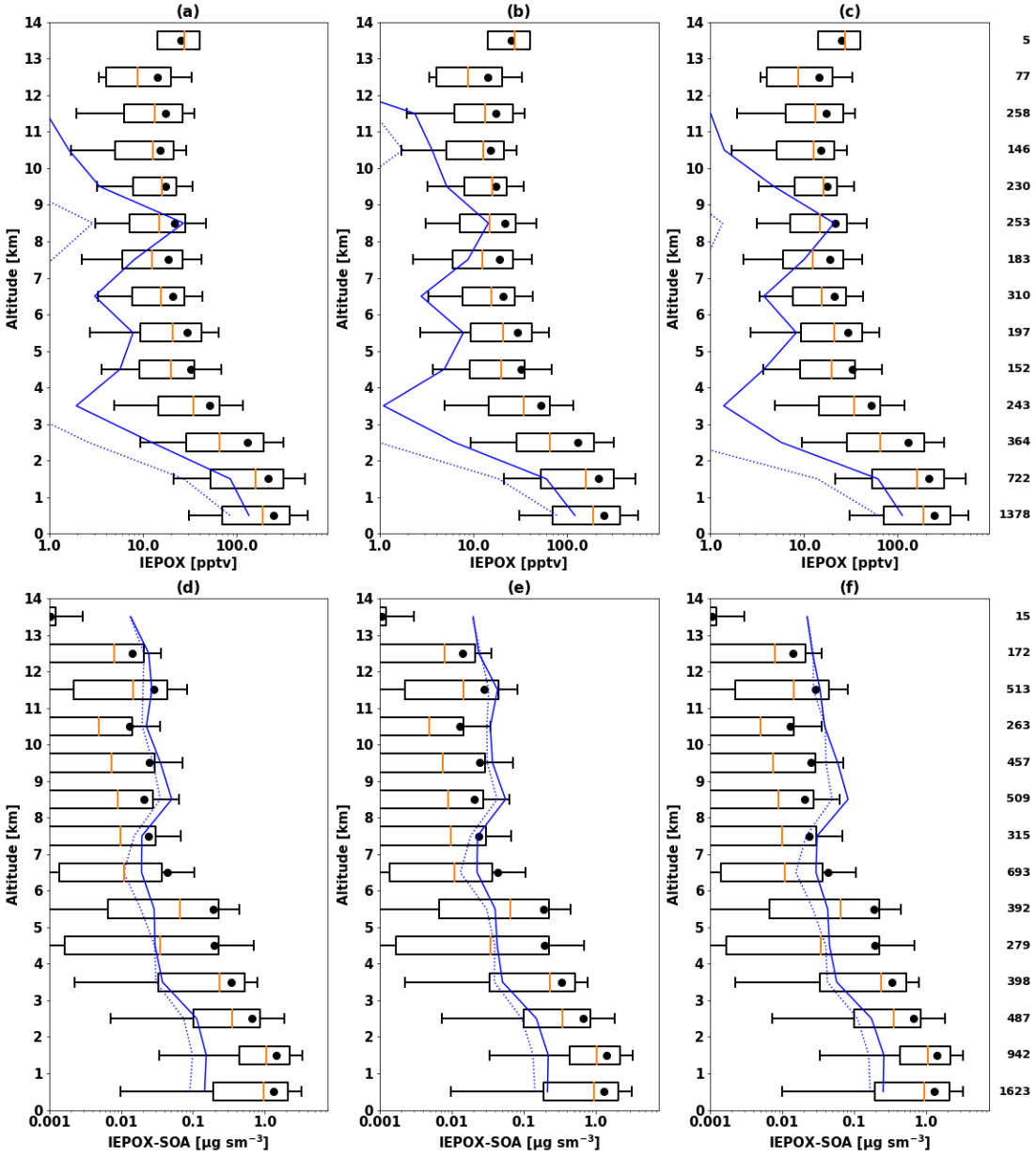

Figure S4. Same as Fig. 1 (c,d) but used different H^* values. 8.5×10^7 , 8.5×10^8, 8.5×10^9 M atm^{-1}, are used for (a,d), (b,e), and (c,f), respectively. SOA yield from IEPOX reactive uptake was assumed to be 0.2. IEPOX comparisons are shown in top panels (a,b,c) and IEPOX-SOA in bottom panels (d,e,f).

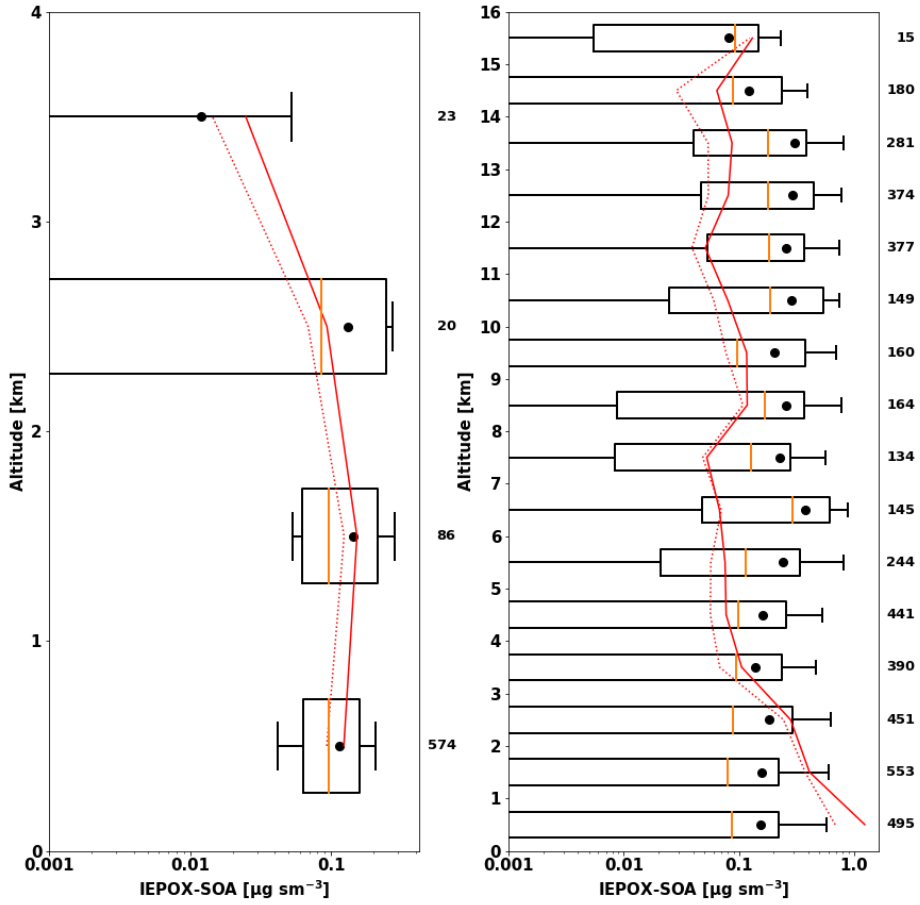

Figure S5. Same as Fig. 2 (c) and (d) but used H^* of 8.5×10^7 M atm^{-1} and the yield of 0.2. The model with the half isoprene emission case (red) is only shown.

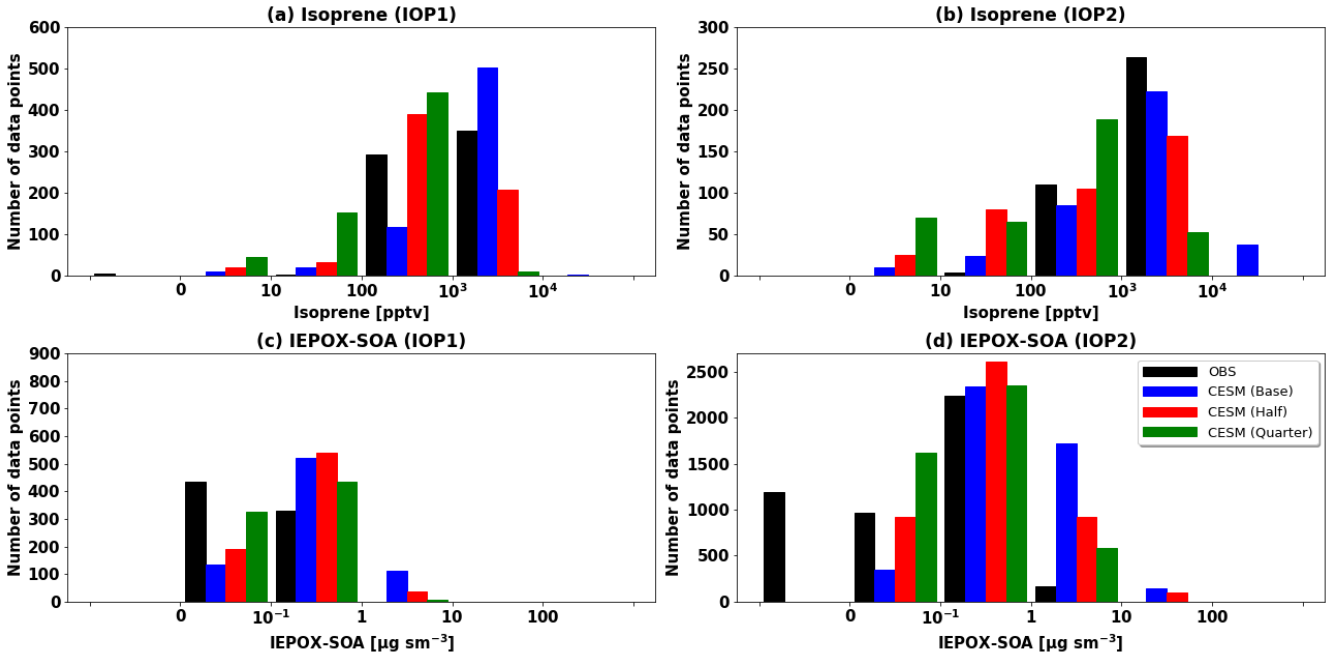

Figure S6. Histograms for observed and modeled (a,b) isoprene and (c,d) IEPOX-SOA concentrations during the GoAmazon campaign. Observations are shown in black bars, and CESM results with different isoprene emissions sensitivities are represented in blue (Base), red (Half), and green (Quarter) bars.

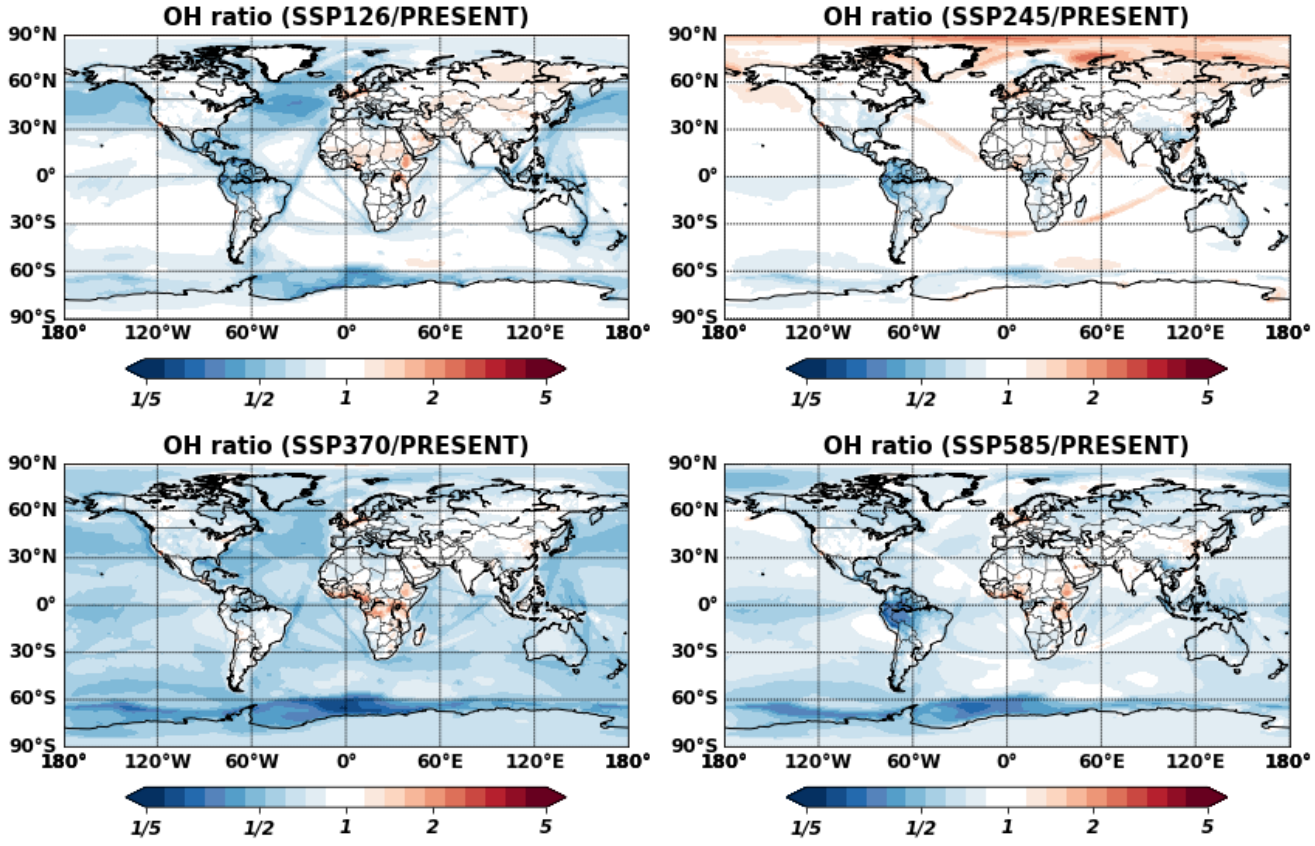

Figure S7. Global ratios of OH simulated under future SSP scenarios (2090s) to present conditions (2010s) at the surface (Explicit case).

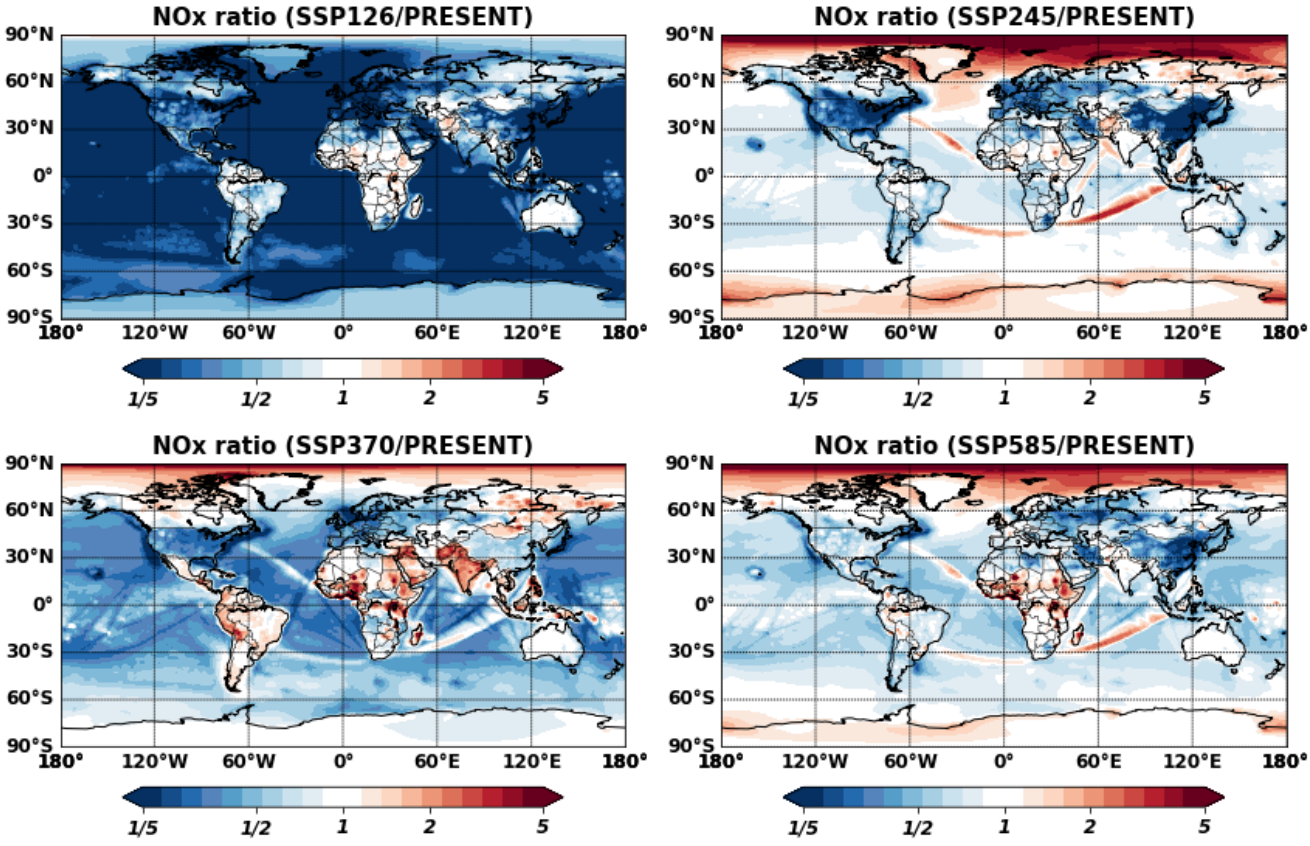

Figure S8. Global ratios of NO_x under future SSP scenarios (2090s) to present conditions (2010s) at the surface (Explicit case).

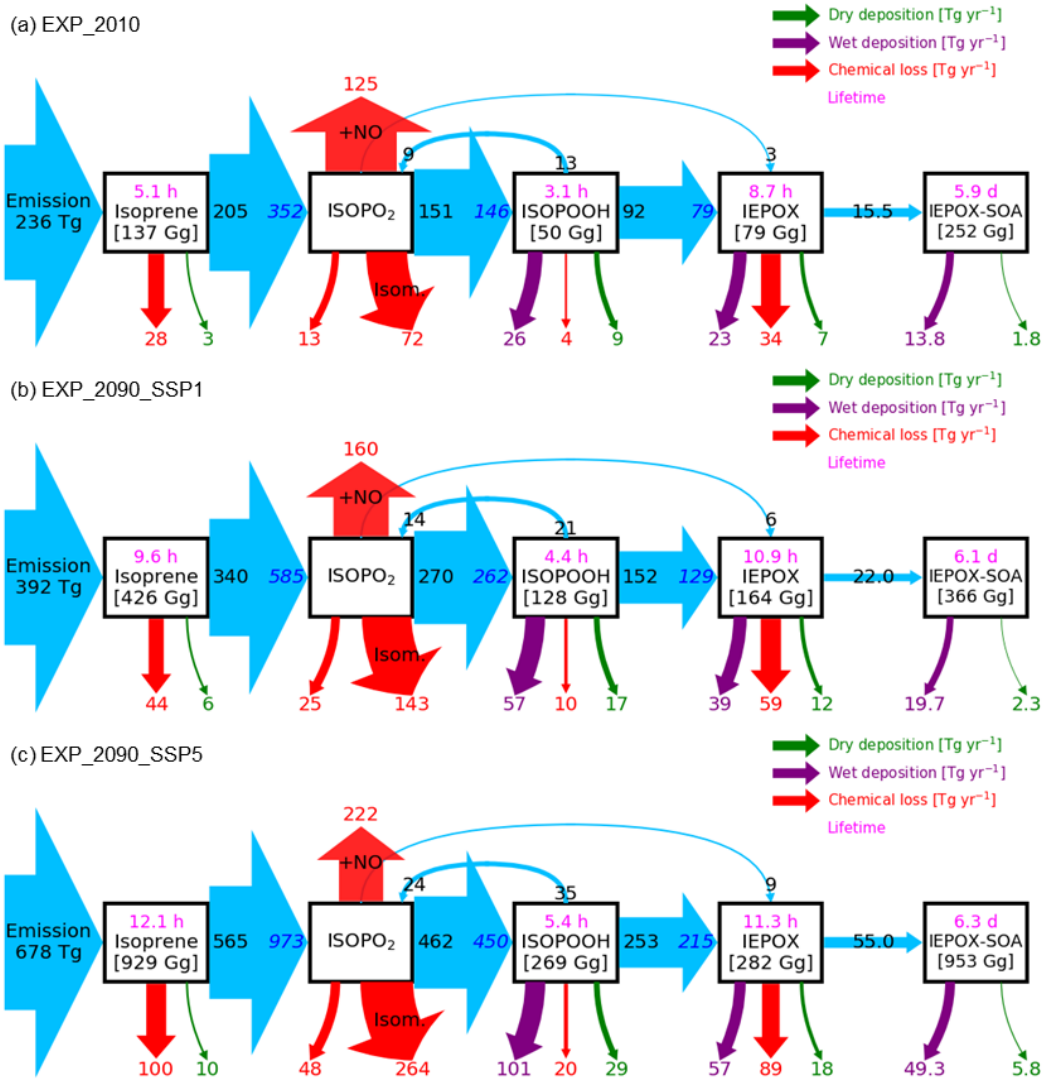

Figure S9. Same as Fig. 6 but for absolute values of mass fluxes (in Tg yr^{-1}).

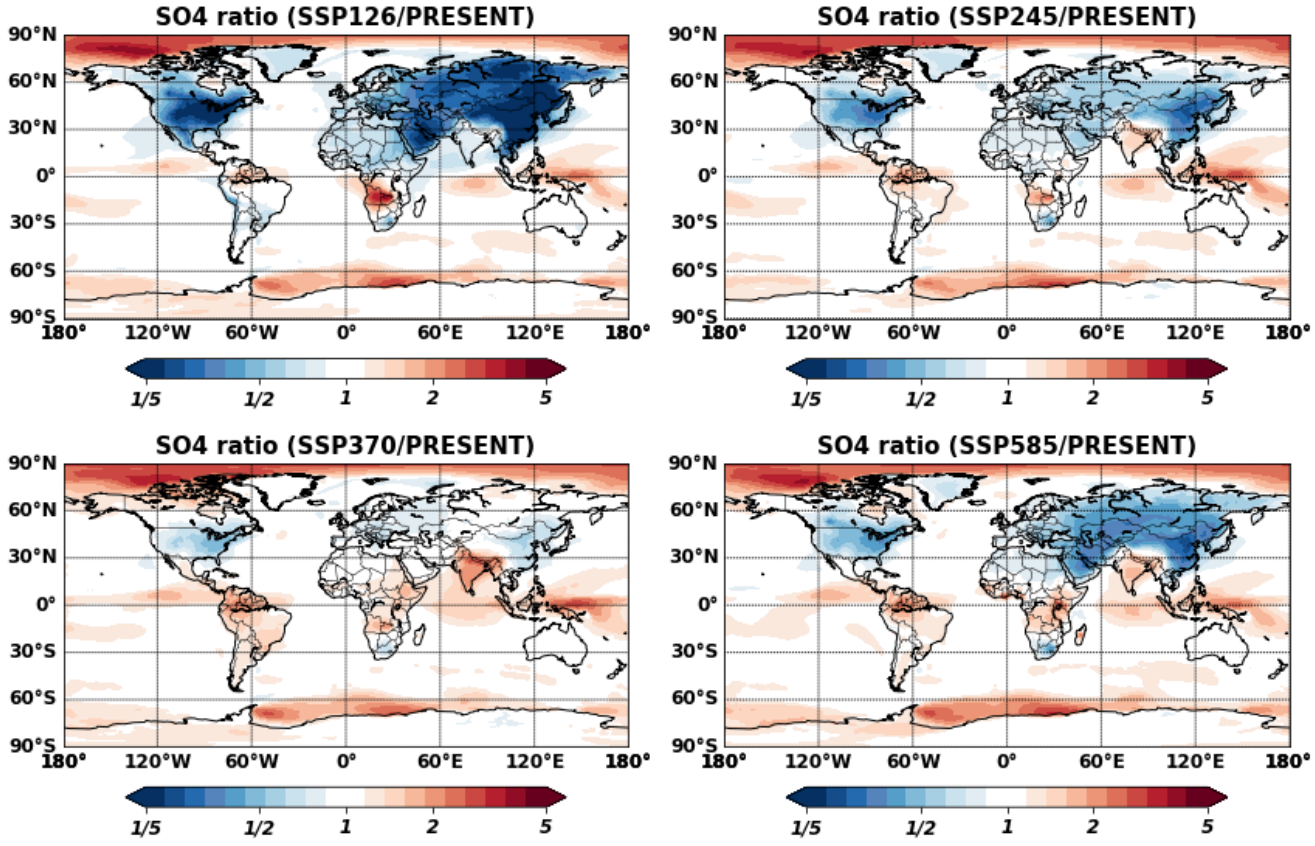

Figure S10. Global ratios of sulfate aerosols under future SSP scenarios (2090s) to present conditions (2010s) at the surface (Explicit case).

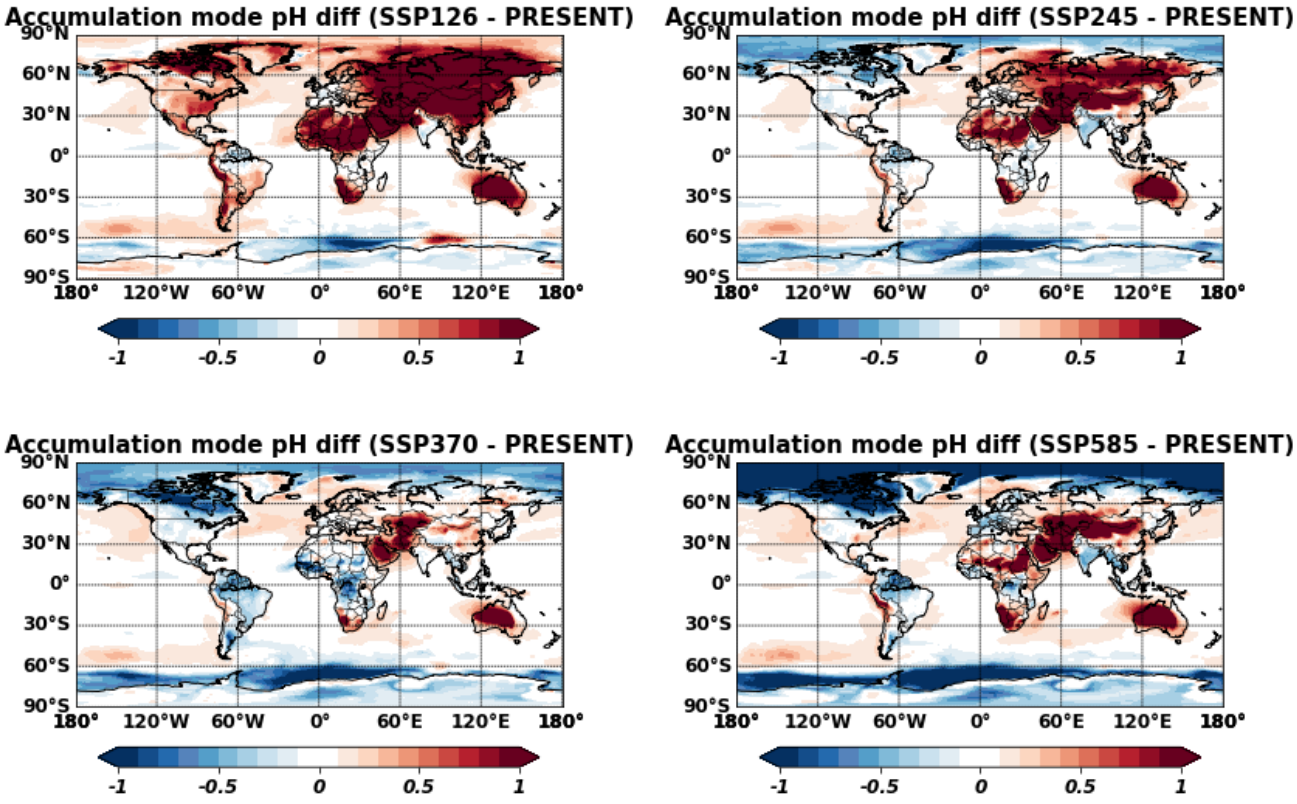

Figure S11. The global aerosol pH (accumulation mode) differences between future SSP scenarios (2090s) and present conditions (2010s) at the surface (Explicit case).

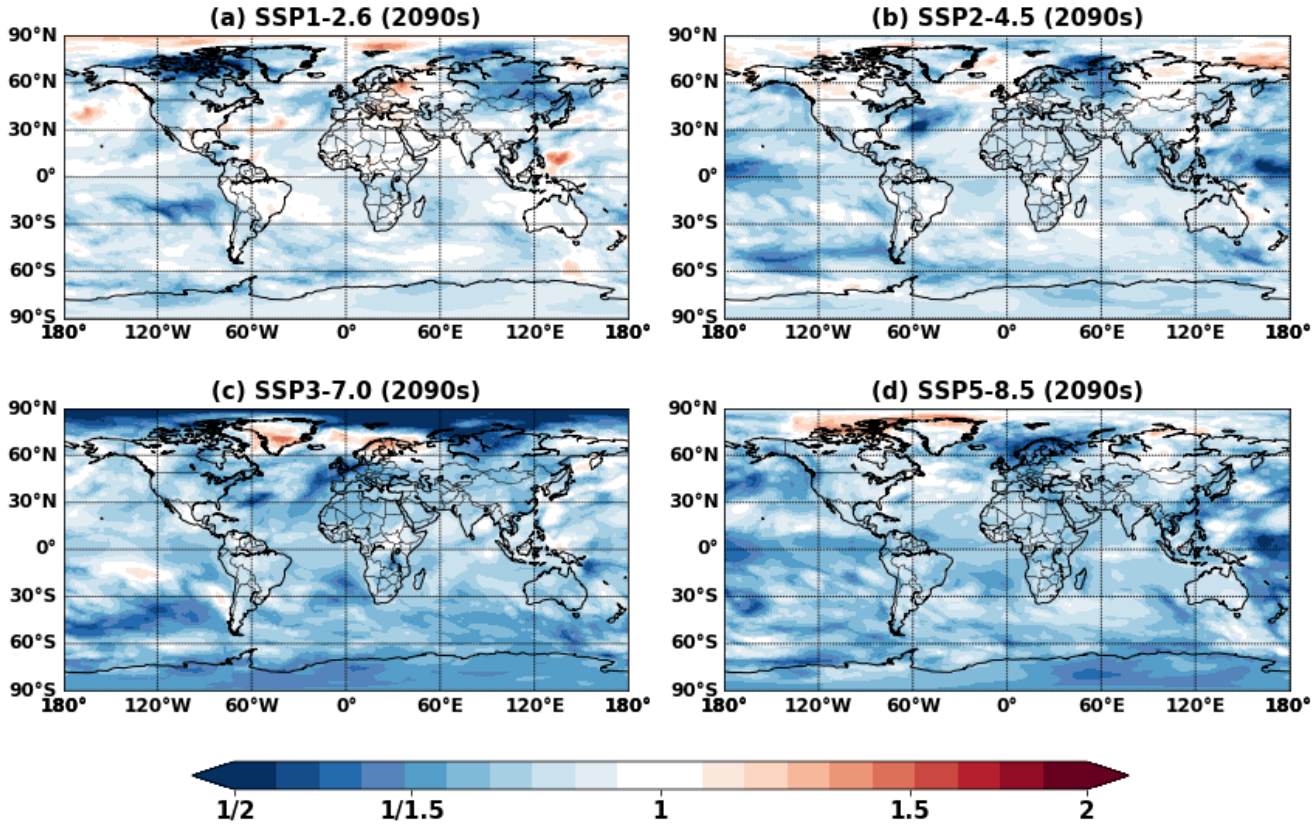

Figure S12. Global ratio maps of surface mean IEPOX-SOA concentrations between EXP_2090_CO2 (with CO_2 inhibition) and EXP_2090 (without CO_2 inhibition) for different SSP scenarios.

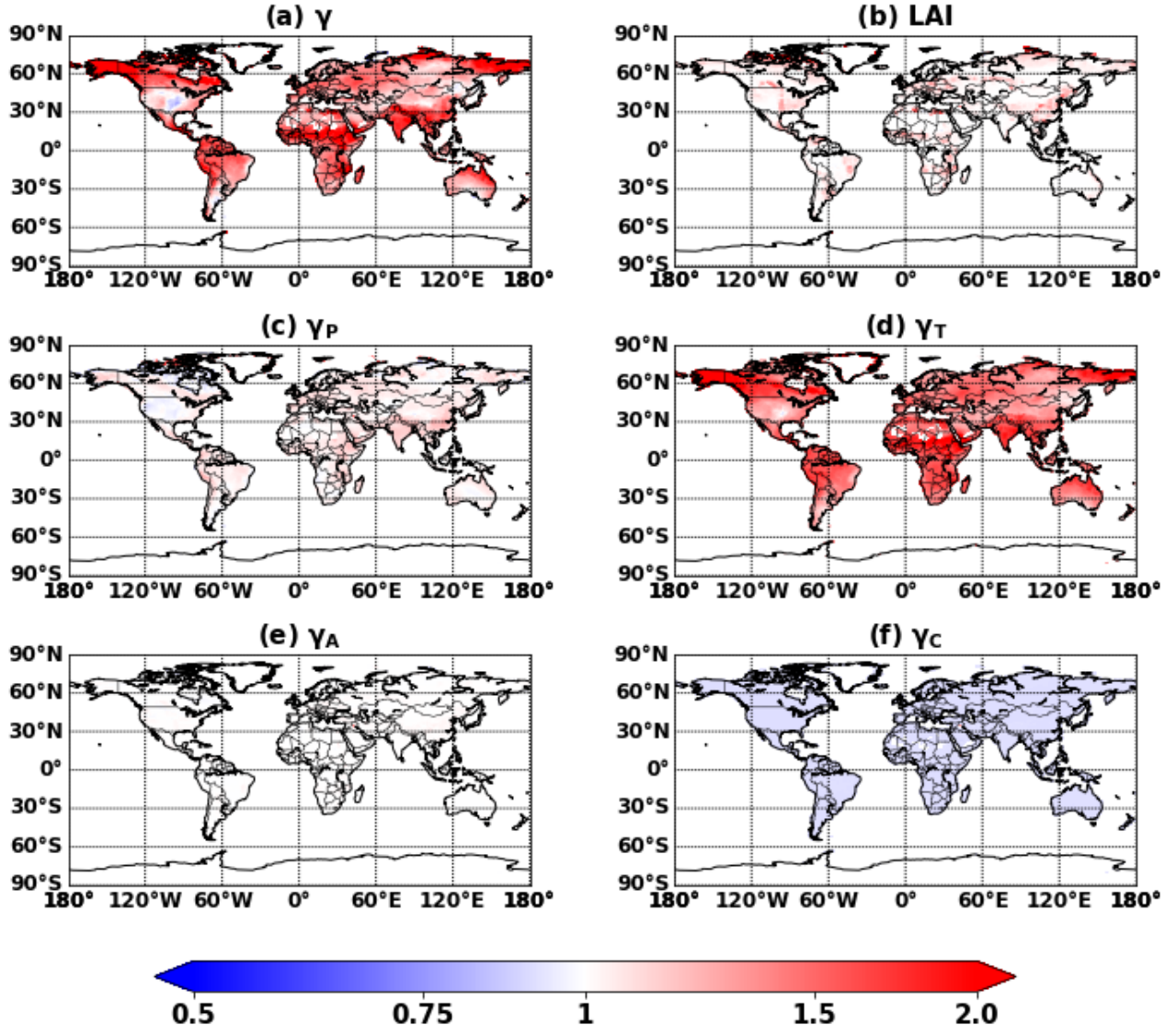

Figure S13. Global maps of activity factor changes (ratio of SSP1-2.6 to present) used in isoprene emission calculations by MEGANv2.1. (a) total activity factor (γ), (b) leaf area index (LAI), (c) emission response to light (γ_P), (d) temperature (γ_T), (e) leaf age (γ_A), and (f) CO_2 inhibition. See Eq. (2) in Guenther et al. (2012) for details. Soil moisture factor is not included, as CESM2.1.0 applies a unity value for soil moisture factor.

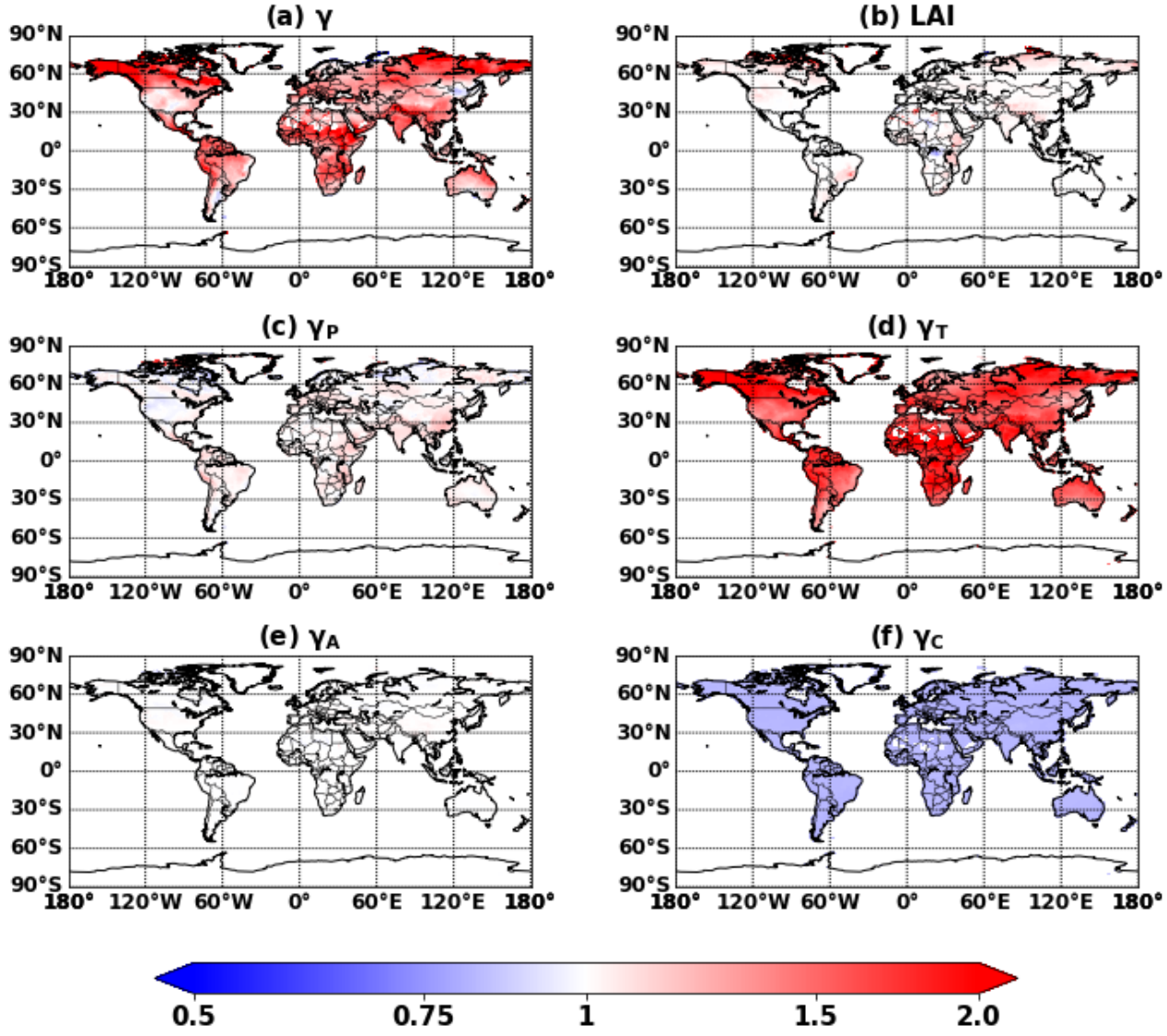

Figure S14. Same as Fig. S13 but for the SSP5-8.5 scenario.

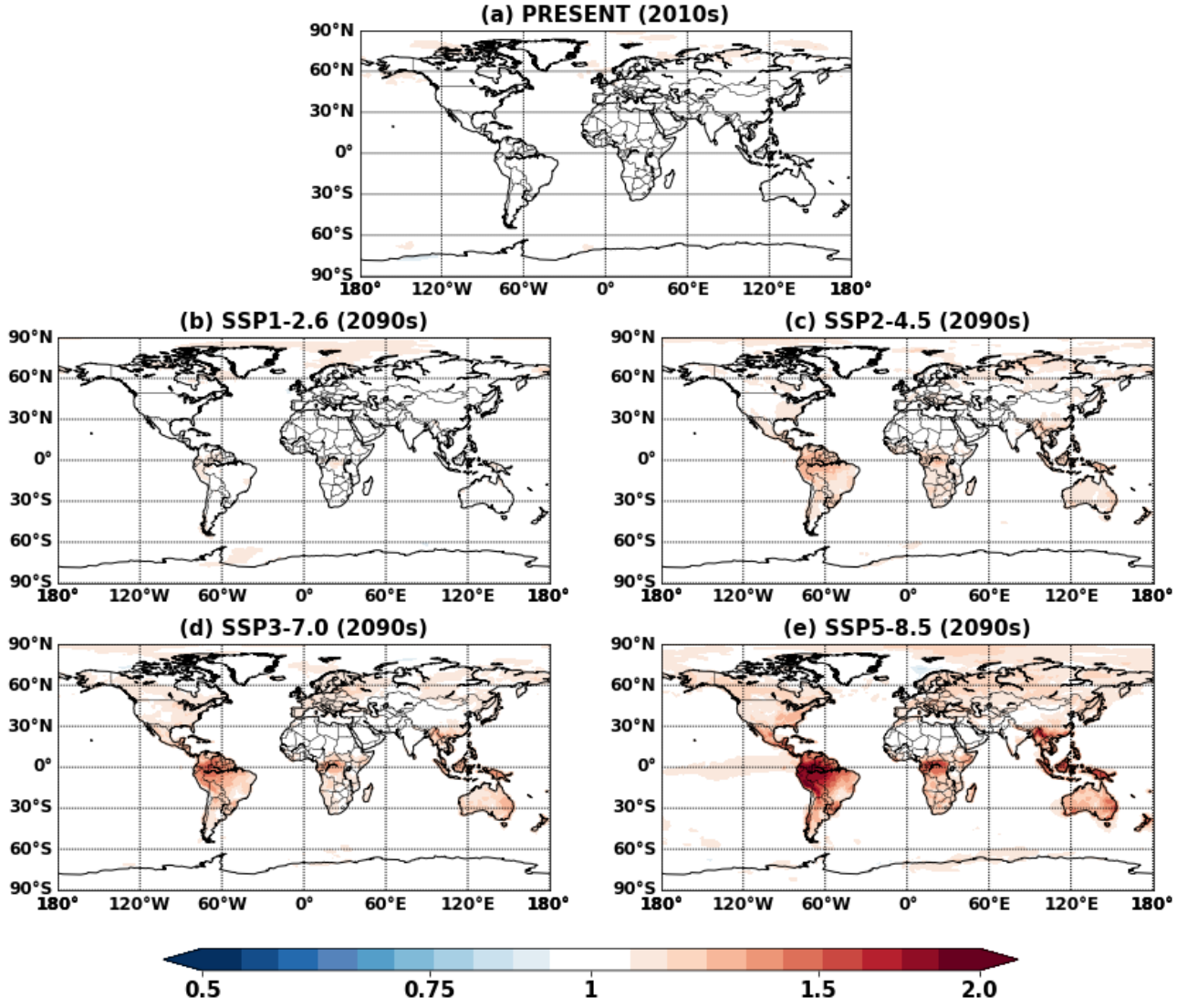

Figure S15. Global ratio maps of OH concentrations between simulations with (EXP) and without CO_2 (EXP_CO2) inhibition effects.

Table S1. Datasets used in Sect. 3.3 and Fig. 4[a]. Ranges or average plus standard deviation of $f_{C_5H_6O}$ (high resolution) and f_{82} (unit mass resolution) in different studies are also included.

Name of datasets	Time Period	Site locations and descriptions	Campaign name	Ranges or average±std.dev. f_{C5H6O} (‰)	Ranges or average±std.dev. f_{82} (‰)	OA Conc. (ug/m3)	IEPOX-SOA Conc. (ug/m3)	IEPOX-SOA/OA (%)	Latitude	longitude	Ref.	X axis in Fig. 4
Studies strongly-influenced by isoprene emissions under lower NO												
SE US forest-CTR site	Jun-Jul, 2013	Centreville, AL	SOAS	6.2±2.4	7.6±2.2	3.8	0.64	17	32.95	-87.13	-1	Centreville 2013
SE US forest-Look Rook site	Jun-Jul, 2013	Look Rook	SOAS	N/A	N/A	4.87	1.6	33	35.61	-83.55	-2	Look Rook 2013
Pristine Amazon forest 2008, Brazil	Feb-Mar, 2008	Pristine rain forest site, TT34	AMAZE-08	5.0±2.3	7.9±1.7	0.76	0.26	34	-2.59	-60.2	-3	Amazon 2008
Amazon forest downwind Manaus, Brazil	Feb-Mar, 2014	T3 site, near Manacapuru	GoAmazon 2014/5	6.9±1.6	7.1±1.0	1.3	0.286	22	-3.21	-60.59	-4	Amazon 2014
Pristine Amazon forest 2014, Brazil	Aug-Dec, 2014	T0 site, ~150 km northeast of Manaus	GoAmazon 2014/5	N/A	5.6±1.7	N/A	N/A	N/A	-3.21	-60.59	-5	N/A
SEAC4RS	Aug-Sep, 2013	Aircraft measurement	SEAC4RS	4.3±1.6	N/A	N/A	N/A	32	Flight track	Flight track	-6	N/A
Borneo forest, Malaysia	Jun-Jul, 2008	Rain forest GAW station, Sabah, Malaysia	OP3	10±0.3	12.4±0.4	0.75	0.18	24	4.981	117.844	-7	Borneo 2008
Atlanta, US	Aug-Sep, 2011	Urban JST site, Atlanta, Georgia, US	N/A	N/A	3.7±1.9	11.6	3.8	33	33.78	-84.42	-8	Atlanta JST 2011
Atlanta (JST), US	May, 2012	Urban JST site, Atlanta, Georgia, US	N/A	3.3±0.9	N/A	9.1	1.91	21	33.78	-84.42	-9	Atlanta JST 2012
Atlanta (GT), US	Aug, 2012	Urban Georgia Tech site, Georgia, US	N/A	5.4±1.9	N/A	9.6	3	31	33.78	-84.396	-9	Atlanta GT 2012
Yorkville, US	July, 2012	Rural sites, 80km northwest of JST site, Georgia, US	N/A	7.7±2.2	N/A	11.2	4	36	33.9285	-85.045	-9	Yorkville 2012
Harrow, Canada	Jun-Jul, 2007	Harrow site, rural sites surrounded by farmland, Canada	BAQSMET	N/A	N/A	N/A	N/A	17	42.03	-82.9	-10	N/A

Bear Creek, Canada	Jun-Jul, 2007	Bear Creek site, wetlands area surrounded by farmland, Canada	BAQSMET	N/A	N/A	N/A	N/A	6	42.51	-82.34	-10	N/A
Studies strongly-influenced by monoterpene emissions												
Rocky mountain pine forest, CO, USA	Jul-Aug, 2011	Manitou Experimental Forest Observatory, CO,	BEACHON-RoMBAS	3.7±0.5	5.1±0.5	N/A	N/A	N/A	39.1	-105.1	-11	N/A
European Boreal forest, Finland	2008-2009	Hyytiala site in Pine forest, Finland	EUCAARI campaign	2.5±0.1 [b]	4.8±0.1 [b]	N/A	N/A	N/A	61.85	24.28	-7	N/A
Studies mixed-influenced by isoprene and monoterpene emissions												
North American temperate, US	Aug-Sep, 2007	Blodgett Forest Ameriflux Site, CA, US	BEARPEX	4.0±<0.1 [b]	4.0±<0.1 [b]	N/A	N/A	N/A	N/A	N/A	-7	N/A
Studies strongly-influenced by urban emissions												
Los Angeles area , CA, USA	May-Jun, 2010	Pasadena, US	CalNex	1.6±0.2	3.6±0.5	7	<DL	< PMF limit	34.14	-118.12	-12	Pasadena 2010
Beijing, China	Nov-Dec, 2010	Peking University, in NW of Beijing city, China	N/A	1.5±0.3	4.6±0.7	34.5	<DL	< PMF limit	39.99	116.31	-13	Beijing 2010
Changdao island, Downwind of China	Mar-Apr, 2011	Changdao island, China	CAPTAIN	1.6±0.2	3.8±0.5	13.4	<DL	< PMF limit	37.99	120.7	-14	Changdao 2011
Barcelona area, Spain	Feb-Mar, 2009	Montseny, Spain	DAURE	1.6±0.2	4.8±0.9	N/A	<DL	< PMF limit	41.38	2.1	-15	Montseny 2009

a- HR-ToF-AMS was used for all the campaigns except the Atlanta, US and Pristine Amazon forest 2014, Brazil using ACSM.

b- Standard error

(1)(Hu et al., 2015); (2)(Budisulistiorini et al., 2015); (3)(Chen et al., 2015); (4)(de Sá et al., 2017); (5)(Carbone et al., 2015); (6)(Liao et al., 2014) ; (7)(Robinson et al., 2011); (8)(Budisulistiorini et al., 2013); (9)(Xu et al., 2015a; Xu et al., 2015b); (10)(Slowik et al., 2011); (11)(Ortega et al., 2014); (12)(Hayes et al., 2013); (13)(Hu et al., 2016); (14)(Hu et al., 2013); (15)(Minguillón et al., 2011)

References

Budisulistiorini, S. H., Canagaratna, M. R., Croteau, P. L., Marth, W. J., Baumann, K., Edgerton, E. S., Shaw, S. L., Knipping, E. M., Worsnop, D. R., Jayne, J. T., Gold, A. and Surratt, J. D.: Real-time continuous characterization of secondary organic aerosol derived from isoprene epoxydiols in downtown Atlanta, Georgia, using the Aerodyne Aerosol Chemical Speciation Monitor, Environ. Sci. Technol., 47(11), 5686–5694, 2013.

Budisulistiorini, S. H., Li, X., Bairai, S. T., Renfro, J., Liu, Y., Liu, Y. J., McKinney, K. A., Martin, S. T., McNeill, V. F., Pye, H. O. T., Nenes, A., Neff, M. E., Stone, E. A., Mueller, S., Knote, C., Shaw, S. L., Zhang, Z., Gold, A. and Surratt, J. D.: Examining the effects of anthropogenic emissions on isoprene-derived secondary organic aerosol formation during the 2013 Southern Oxidant and Aerosol Study (SOAS) at the Look Rock, Tennessee ground site, Atmos. Chem. Phys., 15(15), 8871–8888, 2015.

Carbone, S., De Brito, J. F., Andreae, M., Pöhlker, C., Chi, X., Saturno, J., Barbosa, H., and Artaxo, P.: Preliminary characterization of submicron secondary aerosol in the amazon forest –ATTO station, in preparation, 2015.

Chen, Q., Farmer, D. K., Rizzo, L. V., Pauliquevis, T., Kuwata, M., Karl, T. G., Guenther, A., Allan, J. D., Coe, H., Andreae, M. O., Pöschl, U., Jimenez, J. L., Artaxo, P. and Martin, S. T.: Submicron particle mass concentrations and sources in the Amazonian wet season (AMAZE-08), Atmos. Chem. Phys., 15(7), 3687–3701, 2015.

Hayes, P. L., Ortega, A. M., Cubison, M. J., Froyd, K. D., Zhao, Y., Cliff, S. S., Hu, W. W., Toohey, D. W., Flynn, J. H., Lefer, B. L., Grossberg, N., Alvarez, S., Rappenglück, B., Taylor, J. W., Allan, J. D., Holloway, J. S., Gilman, J. B., Kuster, W. C., de Gouw, J. A., Massoli, P., Zhang, X., Liu, J., Weber, R. J., Corrigan, A. L., Russell, L. M., Isaacman, G., Worton, D. R., Kreisberg, N. M., Goldstein, A. H., Thalman, R., Waxman, E. M., Volkamer, R., Lin, Y. H., Surratt, J. D., Kleindienst, T. E., Offenberg, J. H., Dusanter, S., Griffith, S., Stevens, P. S., Brioude, J., Angevine, W. M. and Jimenez, J. L.: Organic aerosol composition and sources in Pasadena, California, during the 2010 CalNex campaign: AEROSOL COMPOSITION IN PASADENA, J. Geophys. Res. D: Atmos., 118(16), 9233–9257, 2013.

Hu, W., Hu, M., Hu, W., Jimenez, J. L., Yuan, B., Chen, W., Wang, M., Wu, Y., Chen, C., Wang, Z., Peng, J., Zeng, L. and Shao, M.: Chemical composition, sources, and aging process of submicron aerosols in Beijing: Contrast between summer and winter: PM POLLUTION IN BEIJING, J. Geophys. Res. D: Atmos., 121(4), 1955–1977, 2016.

Hu, W. W., Hu, M., Yuan, B., Jimenez, J. L., Tang, Q., Peng, J. F., Hu, W., Shao, M., Wang, M., Zeng, L. M., Wu, Y. S., Gong, Z. H., Huang, X. F. and He, L. Y.: Insights on organic aerosol aging and the influence of coal combustion at a regional receptor site of central eastern China, Atmos. Chem. Phys., 13(19), 10095–10112, 2013.

Hu, W. W., Campuzano-Jost, P., Palm, B. B., Day, D. A., Ortega, A. M., Hayes, P. L., Krechmer, J. E., Chen, Q., Kuwata, M., Liu, Y. J., Sá, S. S. de, McKinney, K., Martin, S. T., Hu, M., Budisulistiorini, S. H., Riva, M., Surratt, J. D., Clair, J. M. S., Isaacman-Van Wertz, G., Yee, L. D., Goldstein, A. H., Carbone, S., Brito, J., Artaxo, P., Gouw, J. A. de, Koss, A., Wisthaler, A., Mikoviny, T., Karl, T., Kaser, L., Jud, W., Hansel, A., Docherty, K. S., Alexander, M. L., Robinson, N. H., Coe, H., Allan, J. D., Canagaratna, M. R., Paulot, F. and Jimenez, J. L.: Characterization of a real-time tracer for isoprene epoxydiols-derived secondary organic aerosol (IEPOX-SOA) from aerosol mass spectrometer measurements, Atmos. Chem. Phys., 15(20), 11807–11833, 2015.

Liao, J., Froyd, K. D., Murphy, D. M., Keutsch, F. N., Yu, G., Wennberg, P. O., St Clair, J. M., Crounse, J. D., Wisthaler, A., Mikoviny, T., Jimenez, J. L., Campuzano-Jost, P., Day, D. A., Hu, W., Ryerson, T. B., Pollack, I. B., Peischl, J., Anderson, B. E., Ziemba, L. D., Blake, D. R., Meinardi, S. and Diskin, G.: Airborne measurements of organosulfates over the continental U.S, J. Geophys. Res. D: Atmos., 120(7), 2990–3005, 2015.

Minguillón, M. C., Perron, N., Querol, X., Szidat, S., Fahrni, S. M., Alastuey, A., Jimenez, J. L., Mohr, C., Ortega, A. M., Day, D. A., Lanz, V. A., Wacker, L., Reche, C., Cusack, M., Amato, F., Kiss, G., Hoffer, A., Decesari, S., Moretti, F., Hillamo, R., Teinilä, K., Seco, R., Peñuelas, J., Metzger, A., Schallhart, S., Müller, M., Hansel, A., Burkhart, J. F., Baltensperger, U. and Prévôt, A. S. H.: Fossil versus contemporary sources of fine elemental and organic carbonaceous particulate matter during the DAURE campaign in Northeast Spain, Atmos. Chem. Phys., 11(23), 12067–12084, 2011.

Ortega, J., Turnipseed, A., Guenther, A. B., Karl, T. G., Day, D. A., Gochis, D., Huffman, J. A., Prenni, A. J., Levin, E. J. T., Kreidenweis, S. M., DeMott, P. J., Tobo, Y., Patton, E. G., Hodzic, A., Cui, Y. Y., Harley, P. C., Hornbrook, R. S., Apel, E. C., Monson, R. K., Eller, A. S. D., Greenberg, J. P., Barth, M. C., Campuzano-Jost, P., Palm, B. B., Jimenez, J. L., Aiken, A. C., Dubey, M. K., Geron, C., Offenberg, J., Ryan, M. G., Fornwalt, P. J., Pryor, S. C., Keutsch, F. N., DiGangi, J. P., Chan, A. W. H., Goldstein, A. H., Wolfe, G. M., Kim, S., Kaser, L., Schnitzhofer, R., Hansel, A., Cantrell, C. A., Mauldin, R. L. and Smith, J. N.: Overview of the Manitou Experimental Forest Observatory: site description and selected science results from 2008 to 2013, Atmos. Chem. Phys., 14(12), 6345–6367, 2014.

Robinson, N. H., Hamilton, J. F., Allan, J. D., Langford, B., Oram, D. E., Chen, Q., Docherty, K., Farmer, D. K., Jimenez, J. L., Ward, M. W., Hewitt, C. N., Barley, M. H., Jenkin, M. E., Rickard, A. R., Martin, S. T., McFiggans, G. and Coe, H.: Evidence for a significant proportion of Secondary Organic Aerosol from isoprene above a maritime tropical forest, Atmos. Chem. Phys., 11(3), 1039–1050, 2011.

Sá, S. S. de, Palm, B. B., Campuzano-Jost, P., Day, D. A., Newburn, M. K., Hu, W., Isaacman-VanWertz, G., Yee, L. D., Thalman, R., Brito, J., Carbone, S., Artaxo, P., Goldstein, A. H., Manzi, A. O., Souza, R. A. F., Mei, F., Shilling, J. E., Springston, S. R., Wang, J., Surratt, J. D., Alexander, M. L., Jimenez, J. L. and Martin, S. T.: Influence of urban pollution on the production of organic particulate matter from isoprene epoxydiols in central Amazonia, Atmos. Chem. Phys., 17(11), 6611–6629, 2017.

Slowik, J. G., Brook, J., Chang, R. Y.-W., Evans, G. J., Hayden, K., Jeong, C.-H., Li, S.-M., Liggio, J., Liu, P. S. K., McGuire, M., Mihele, C., Sjostedt, S., Vlasenko, A. and Abbatt, J. P. D.: Photochemical processing of organic aerosol at nearby continental sites: contrast between urban plumes and regional aerosol, Atmos. Chem. Phys., 11(6), 2991–3006, 2011.

Xu, L., Suresh, S., Guo, H., Weber, R. J. and Ng, N. L.: Aerosol characterization over the southeastern United States using high-resolution aerosol mass spectrometry: spatial and seasonal variation of aerosol composition and sources with a focus on organic nitrates, Atmos. Chem. Phys., 15(13), 7307–7336, 2015a.

Xu, L., Guo, H., Boyd, C. M., Klein, M., Bougiatioti, A., Cerully, K. M., Hite, J. R., Isaacman-VanWertz, G., Kreisberg, N. M., Knote, C., Olson, K., Koss, A., Goldstein, A. H., Hering, S. V., de Gouw, J., Baumann, K., Lee, S.-H., Nenes, A., Weber, R. J. and Ng, N. L.: Effects of anthropogenic emissions on aerosol formation from isoprene and monoterpenes in the southeastern United States, Proc. Natl. Acad. Sci. U. S. A., 112(1), 37–42, 2015b.